

Spin flip scattering at Al surfaces.

N. Poli* and M. Urech, V. Korenivski, D. B. Haviland

Nanostructure Physics, Royal Institute of Technology,

Albanova University Centre, SE-10691 Stockholm, Sweden

Non-local measurements are performed on a multi terminal device to *in – situ* determine the spin diffusion length and in combination with resistivity measurements also the spin relaxation time in Al films. By varying the thickness of Al we determine the contribution to spin relaxation from surface scattering. From the temperature dependence of the spin diffusion length it is established that the spin relaxation is impurity dominated at low temperature. A comparison of the spin and momentum relaxation lengths for different thicknesses reveals that the spin flip scattering at the surfaces is weak compared to that within the bulk of the Al films.

PACS numbers:

The first experiment on spin injection and detection in metals dates back to 1985 when Johnson and Silsbee [1, 2] demonstrated spin accumulation in a single-crystal Al for temperatures below 77 K, with a spin diffusion length, $\lambda_{sf} \sim 100 \mu m$. Recent experiments on thin films [3, 4, 5, 6, 15] found orders of magnitude shorter $\lambda_{sf} \sim 0.1 - 1 \mu m$. However, the measured spin accumulation is greatly enhanced due to much reduced effective device volumes. Understanding the origins of spin relaxation in such devices is therefore important for spintronics applications. The main contribution to spin relaxation in a metal is the spin

*Electronic address: poli@kth.se

orbit coupling induced by the lattice ions in the metal [7, 8]. In combination with momentum scattering, spin flip events can occur with a certain (typically small) probability, which depends on the specific band structure, nature of the impurities present, phonons, etc. As the dimensions of electronic devices decrease, the influence of surface scattering becomes important. We analyze this contribution by studying the temperature and thickness dependence of spin relaxation parameters in thin Al films. We find that the spin relaxation is impurity dominated at low temperatures (LT) and, surprisingly, that the spin flip scattering at the surfaces is negligible compared to that within the bulk.

Multi terminal lateral devices allow several simultaneous measurements to be conducted. For example, the spin imbalance in a non-magnetic metal (NM) produced by current injection from a ferromagnet (FM) can be detected at various distances from the injection point using a set of magnetic electrodes, as illustrated in Figure 1. Thus, detecting voltages non-locally (outside the current path) at two or more locations of the Al strip allows an in-situ determination of λ_{sf} [15]. The non-equilibrium spin accumulation produced at the injection point diffuses along the Al, governed by the diffusion equation,

$$\nabla^2 \delta\mu = \delta\mu / \lambda_{sf}^2, \quad (1)$$

where $\delta\mu = (\mu_{\uparrow} - \mu_{\downarrow})$ is the spin splitting in the chemical potential, $\lambda_{sf} = \sqrt{D\tau_{sf}}$, and D is the diffusion constant given by the Einstein relation, $\sigma = e^2ND$. The solution of (1) with appropriate boundary conditions gives the "spin signal" at a distance x from the injection point

$$R_x = \frac{\Delta V}{I_{inj.}} = P^2 \frac{\rho \lambda_{sf}}{A} e^{-x/\lambda_{sf}}, \quad (2)$$

where P is the polarization of the injector, ρ and A are the resistivity and the cross sectional area of the NM, respectively.

The resistivity of a metal is expected to increase rapidly when the thickness of the metal becomes comparable to or smaller than the mean free path. This increase is due to scattering at surfaces [9, 10, 11] and grain boundaries [12]. These two contributions were considered by Sables' [13] who assigned an angle dependent specularity $p_i(\cos \theta)$ to each surface and assumed columnar grain growth, with the average grain diameter D and grain boundary specularity R . The result of this model for the ratio of the bulk resistivity ρ_0 to the total resistivity ρ_{tot} can be expressed as a function of the film thickness normalised to the bulk mean free path ($k = d/\lambda_0$)

$$\frac{\rho_0}{\rho_{tot}} = G(\alpha) - \frac{4}{\pi} \int_0^{\frac{\pi}{2}} d\phi \int_0^1 du \cos^2 \phi 3(u - u^3) \times \quad (3)$$

$$\frac{\{1 - \exp(-kH/u)\} \{1 - \bar{p} + (\bar{p} - p_1 p_2) \exp(-kH/u)\}}{2kH^2 \{1 - p_1 p_2 \exp(-2kH/u)\}},$$

where

$$G(\alpha) = 1 - \frac{3}{2}\alpha + 3\alpha^2 - 3\alpha^3 \ln \left(1 + \frac{1}{\alpha} \right),$$

$$H = 1 + \frac{\alpha}{\sqrt{(1 - u^2) \cos \phi}},$$

$\alpha = R/(1 - R) \cdot l_0/D$ and $\bar{p} = \frac{1}{2}(p_1 + p_2)$. Using this model, we analyze the relative contributions of the surface and grain boundary scattering to the resistivity of our Al films.

The samples were fabricated using electron beam lithography and the standard two angle deposition technique in an e-gun evaporation system. First, 40 μm long and 100 nm wide Al strips with different thicknesses were deposited at normal incidence, followed by oxidation in O_2 at a pressure of 80 mTorr for 8 min. Oxidation was performed at RT , providing an Al_2O_3 tunnel barrier with a typical specific resistance of $\sim 0.15 \text{ k}\Omega\mu\text{m}^2$. Next, Co electrodes of 50-80 nm in thickness were deposited from an angle of 40° to overlap the Al strip. The Co electrodes are designed to have different widths, between 60 and 70 nm, which results in

different coercive fields, allowing us to switch their magnetization independently. Figure 1 shows a SEM micrograph of the device consisting of 3 vertical Co electrodes, each separated by a distance of 300 nm, overlapping an oxidized Al strip.

To isolate the spin signal, non-local measurements [2] were performed according to the electrical arrangement shown in Figure 1. This allowed us to *in-situ* determine λ_{sf} and, combined with four point resistivity measurements, also τ_{sf} . A bias current of 1 μA was injected into the Al strip and the voltages at the detectors 1 and 2 outside the current path were measured simultaneously using a standard lock-in technique at 7 Hz. High input impedance ($\sim 10^{15} \Omega$) voltage pre-amplifiers with low input bias current (1-10 fA) were used to minimize the noise and current leakage. An external magnetic field was applied in the plane along the length of the FM electrodes in order to switch the magnetizations to the desired states. The measurements were performed for a set of samples having different Al thickness.

Figure 2 shows the spin signals at the two detectors as a function of the external magnetic field for a sample with 15 nm thick Al measured at 4 K. To begin with, all the electrodes were saturated in the negative direction ($\downarrow\downarrow\downarrow$) and then switched separately by ramping the field in the positive direction. First, detector 1 switches ($\downarrow\uparrow\downarrow$) at 1240 Oe, then detector 2 ($\uparrow\uparrow\downarrow$) at 1675 Oe. Finally the injector switches ($\uparrow\uparrow\uparrow$) at 1840 Oe, which one can see as a simultaneous transition in both curves of Figure 2. The measured spin signals at two distances, together with equation 2 gives $P = 12\%$ and $\lambda_{sf} = 660$ nm. Note that both properties were obtained *in-situ* in one field sweep, which eliminates uncertainties due to irreproducibilities in fabrication. We note, that this P value is the effective spin polarization of the injecting interface and is not equal to the bulk polarization of Co (see also [17]).

The temperature dependence of λ_{sf} for the sample with 15 nm thick Al strip is shown

in Figure 3. As T is lowered λ_{sf} increases from ≈ 350 nm at RT until it levels off at ≈ 660 nm at LT , which demonstrates that the spin relaxation is impurity dominated at LT . The data reveals a contribution from phonon mediated scattering, which significantly reduces λ_{sf} for $T > 50$ K. The analysis of the temperature dependence of the resistivity (not shown) reveals that both the diffusion constant and spin relaxation time increase with lowering temperature. Our results on the temperature dependence can be reconciled with the early single crystal data [1, 2] using the theory of [14]. The sole difference appears to be the greater amount of impurities in thin films.

Figure 4 shows the resistivity of the Al films measured at 4 K as a function of thickness together with a theoretical fit according to Eq. 3. The line represents the theoretical prediction of ρ_{tot} for the grain size $D \approx 6$ nm, which was determined by AFM measurements of the topography of the films. The fact that the grain size essentially does not change with thickness results in approximately constant background to the total resistivity from grain boundary scattering. Thus, the dominating contribution to the resistivity of the thinnest films is the diffusive scattering at the surfaces.

To investigate how the additional surface momentum scattering affects spin relaxation, the thickness dependence of λ_{sf} and λ_p at 4 K was determined, where λ_p is the thickness dependent mean free path determined by the measured resistivity. In the bulk limit, where the thickness is greater than both λ_{sf} and λ_p , the ratio of the two should be constant and is estimated to be ≈ 15 . The bulk λ_0 is obtained by extrapolation in Figure 4 to large thicknesses, and the bulk λ_{sf} is estimated from the analysis of the spin relaxation time (to be published elsewhere). In thin films, surface scattering determines λ_p . If the surface scattering contribution to spin relaxation is equally strong as that of the bulk impurity scattering, then the ratio of the two characteristic lengths should be independent of thickness. However, the

measured data for λ_{sf}/λ_p , plotted in Figure 5, shows a clear increase for small thickness. This means that the spin flip scattering at the surfaces is weak compared to the spin relaxation within the bulk of the films. Seen from a perspective of "spin hot spots"

Spin relaxation in Al sensitively depends on the details of the band structure (the so-called "spin hot spots", [14]). It is then natural to expect that the bulk electronic structure is significantly perturbed at the surfaces in such a way that the spin-flip scattering cross-sections are reduced. This provides a qualitative explanation for the weak spin relaxation at the surface we observe.

In conclusion, we have measured the spin relaxation length in Al films as a function of temperature and thickness. We observe that the spin relaxation is dominated by impurity scattering at LT . Interestingly, the contribution from surface scattering to spin relaxation is found to be weak compared to spin relaxation within the bulk of the film.

N. Poli and M. Urech gratefully acknowledge support from the Swedish SSF. We thank John Slonczewski for fruitful discussions.

-
- [1] D. Lubzens and S. Schultz, Phys. Rev. Lett., **36**, 1104 (1976)
- [2] M. Johnson and R. H. Silsbee, Phys. Rev. Lett., **55**, 1790 (1985)
- [3] J. Bass and W. P. Pratt, J. Magn. Magn. Mater. **200**, 274 (1999).
- [4] F. J. Jedema *et al*, Nature, **410**, 345 (2001)
- [5] F. J. Jedema *et al*, Nature, **416**, 713 (2002)
- [6] F. J. Jedema *et al*, Phys. Rev B, **67**, 085319 (2003)
- [7] R. J. Elliot, Phys. Rev. **96**, 266 (1954).
- [8] Y. Yafet, in *Solid state physics*, **14**, (1963)
- [9] K. Fuchs, Proc. Cambridge Philos. Soc. **34**, p. 100 (1938)
- [10] E. H. Sondheimer, Adv. Phys. **1**, p. 1 (1952)
- [11] S. B. Soffer, J. Appl. Phys. **38**, 1710 (1967)
- [12] A. F. Maydas and M. Shatzkes, Phys. Rev. B **1**, 1382 (1970)
- [13] J. R. Sambles, Thin Solid Films **106**, 321 (1983)
- [14] J. Fabian and S. Das Sarma, Phys. Rev. Lett., **83**, 1211 (1999)
- [15] M. Urech, J. Johansson, V. Korenivski and D. B. Haviland, J. Magn. Magn. Mater. **272-276**, e1417 (2004)
- [16] C. R. Tellier and A. J. Tosser, Thin Solid Films **37**, 207 (1976)
- [17] S. O. Valenzuela and M. Tinkham, App. Phys. Lett. **85**, 5914 (2004)

Figure captions

1. Scanning electron micrograph of a multi terminal device. The vertical Co electrodes are in contact with the Al strip through tunnel barriers (Al_2O_3).
2. Spin voltages versus applied magnetic field for a 15 nm Al sample measured at 4K: at detector 1 (upper panel); detector 2 (lower panel). The arrows indicate the magnetic states of the electrodes.
3. Spin diffusion length, λ_{sf} , as a function of temperature for a 15 nm Al sample. At high temperatures, the dominant scattering mechanism is with phonons, whereas it is with impurities at LT ($T < 50$ K).
4. Resistivity of Al films as a function of thickness. The solid line is a theoretical fit for ρ_{tot} with $D \approx 6$ nm, $R \approx 0.1$, $\rho_0 \approx 0.2 \mu\Omega$ cm, $\lambda_0 \approx 200$ nm and maximal surface diffusivities.
5. The ratio of the spin diffusion length and the momentum mean free path as a function of the Al film thickness at 4 K.

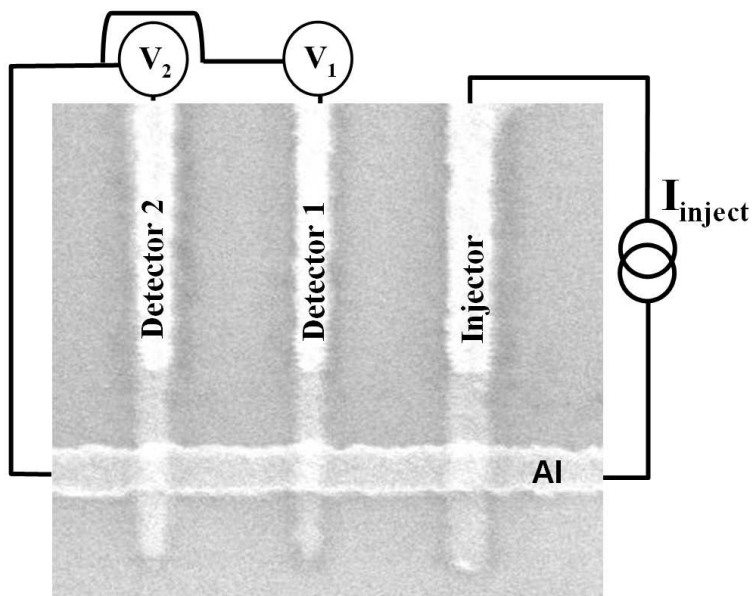


Figure 1: Poli et Al

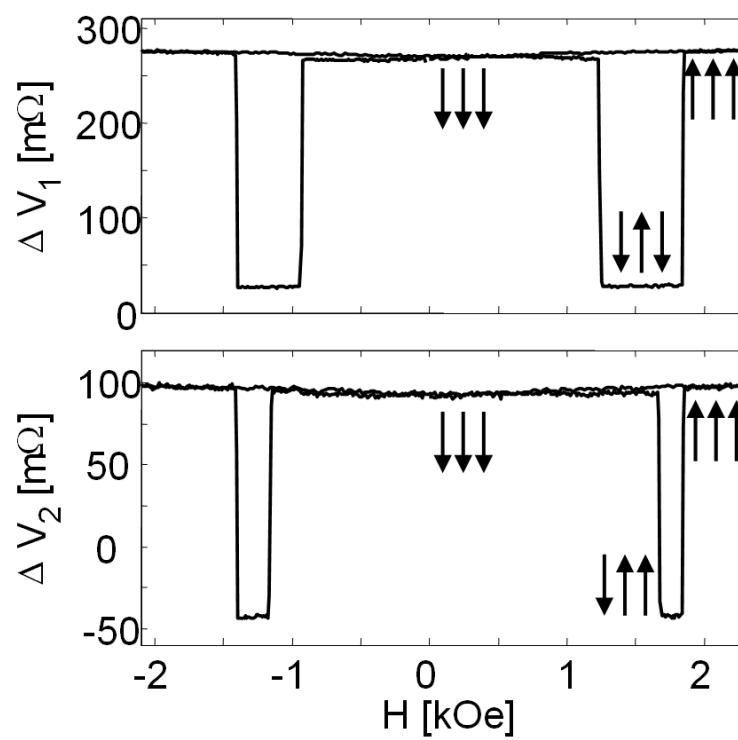


Figure 2: Poli et Al

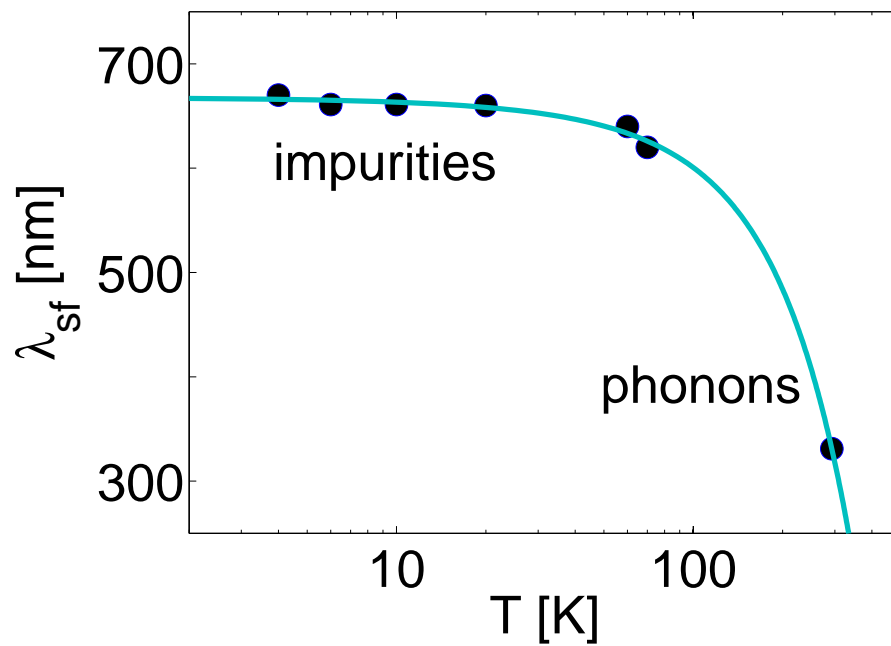


Figure 3: Poli et Al

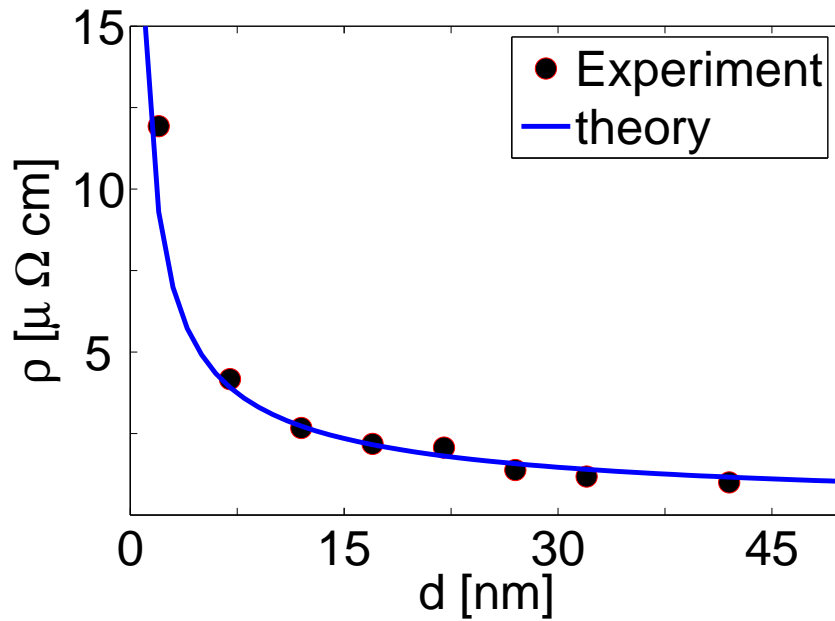


Figure 4: Poli et Al

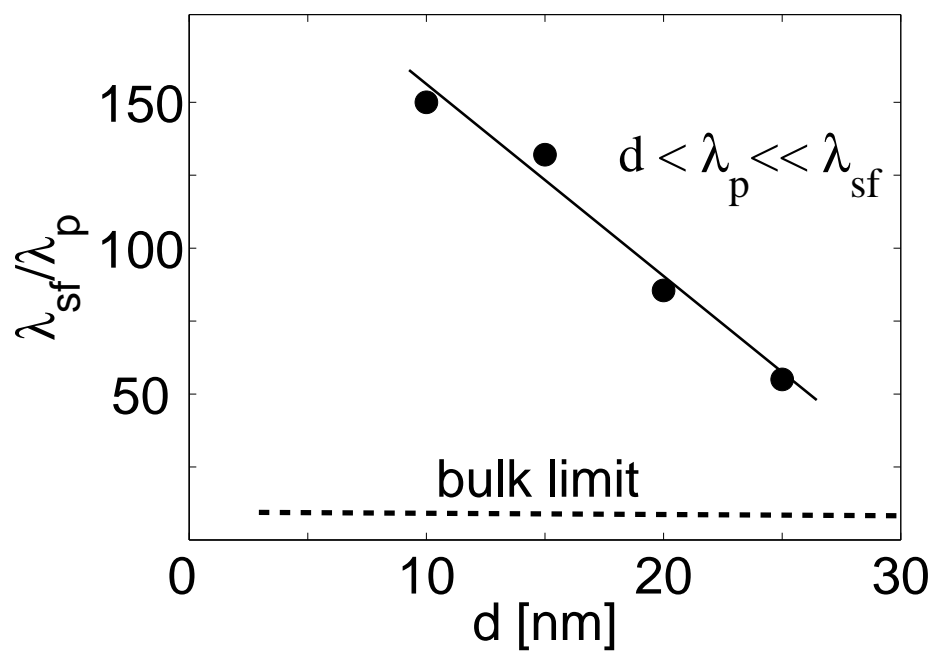


Figure 5: Poli et Al